21cm Intensity Mapping + kSZ Effect: a Handy Probe for Larger Scale, Wider Redshift Baryon Distributions

Dongzi Li,[1,2] Ue-Li Pen,[3,4,5,1] Hong-Ming Zhu,[6,7] and Yu Yu[8]

[1] *Perimeter Institute for Theoretical Physics, 31 Caroline St. N., Waterloo, ON, N2L 2Y5, Canada*
[2] *University of Waterloo, 200 University Ave W, Waterloo, ON, N2L 3G1, Canada*
[3] *Canadian Institute for Theoretical Astrophysics, 60 St. George Street, Toronto, Ontario M5S 3H8, Canada*
[4] *Dunlap Institute for Astronomy and Astrophysics, 50 St. George Street, Toronto, Ontario M5S 3H4, Canada*
[5] *Canadian Institute for Advanced Research, CIFAR Program in Gravitation and Cosmology, Toronto, Ontario M5G 1Z8, Canada*
[6] *Key Laboratory for Computational Astrophysics, National Astronomical Observatories, Chinese Academy of Sciences, 20A Datun Road, Beijing 100012, China*
[7] *University of Chinese Academy of Sciences, Beijing 100049, China*
[8] *Key laboratory for research in galaxies and cosmology, Shanghai Astronomical Observatory, Chinese Academy of Sciences, 80 Nandan Road, Shanghai 200030, China*

(Dated: December 18, 2016)

The prominent defficiency of baryon contents in observations for $z \lesssim 2$ and its close correlation with feedbacks and intergalactic medium conditions stand in the way of understanding structure evolution. To study the distribution of diffusive 'missing baryons', a large scale oriented probe, the kinematic Sunyaev-Zel'dovich (kSZ) effect on cosmic microwave background, was proposed. However, its faintness and lack of redshift require another signal to cross correlate with it. Previous proposals usually require galaxy spectroscopic surveys and new generation ground based CMB experiments to obtain convincing S/N. This induces constraints on redshift depth and sky coverage, and limit the study for scales larger than $\ell < 2000$. In this paper, a new possibility of cross correlating kSZ with HI density from 21cm intensity mapping is discussed. Ongoing intensity mapping experiments, such as CHIME, making use of all weak sources, are able to cover large sky area and consistently measure $z \lesssim 2.5$ sky in next few years. This enable us to study structure evolution of $\ell \sim 1000 - 2000$, which is the scale of clusters and filaments. The greatest challenge for the method is the loss of large scale modes in 21cm intensity mapping due to both foregrounds and spatial loss of inteferometers. we alleviate the problem by applying nonlinear tidal reconstruction to restore the modes. A minimum of 15 S/N for both redshift 1 and 2 could be reached with CHIME + Planck. The fast construction of interferometers with longer baselines, such as HIRAX, may foster the S/N to reach 50 for redshift 2 with noise level of Planck.

PACS numbers:

I. INTRODUCTION

For $z \lesssim 2$, large fractions of predicted baryon contents are missing in observations. The majority of them are believed to reside in warm-hot intergalactic mediums (WHIM) with typical temperature of 10^5 K to 10^7 K [1, 2]. The high temperature and low density impose difficulties on direct detection. Besides, the uncertainties in ionization states, metalicities and pressure lead to confusions on interpreting signals from absroption lines and soft X-rays. It is expected urgently for probes that not only trace the majority of the baryons, but also can be interpreted model-independently.

Among proposed probes, the kinematic Sunyaev-Zel'dovich (kSZ) effect [3–5] is a promising one. kSZ effect results from Compton scattering of cosmic microwave background (CMB) off free electrons. The radial velocity of electrons will give photon a Doppler shift and hence leads to a secondary anisotropy in CMB temperature. It is an ideal probe to tackle the problem: First, it contributes from all the free electrons, and hence contains information about $> 90\%$ of baryons which are in ionized states. Second, the signal is mainly influenced by electron density and radial velocity, regardless the temperature, pressure and metalicity, so no extra assumptions are needed to estimate baryon abundance. Third, the peculiar velocity is dominantly related to large scale structures, therefore the signal is less biased towards local mass contractions, and more indicative about diffusive distributions.

Attractive as it is, two drawbacks largely reduce the feasibility of harnessing kSZ signal. First, the signal is weak and hence suffers seriously from contaminations from primary CMB, facility noises, thermal SZ effect, CMB lensing, etc. Second, it is an integrated effect along line of sight, therefore, kSZ itself does not contain redshift information.

A straight-forward mitigation of the disadvantages is to cross correlate kSZ signal with another tracer, which has both large scale structure and redshift information. Previous work has proposed optical spectroscopic survey as an ideal tool [6–8]. However, lack of prominent spectral lines at redshift $1.4 - 2.5$ makes it difficult to consistently measure evolution from $z > 2$ to $z = 0$. Moreover, the high requirements on facilities and sources largely constraint the sky coverage it could reach, especially when redshift goes up, which limits it to relatively small angular scales, with very low level of primary CMB. Methods trying to relax requirements on density fields, such as cross correlating photo-z galaxies with kSZ [9, 10], depend on models of velocity fields and demand next generation CMB facilities, such as ACTpol, CMB-S4, to achieve convincing S/N.

In this paper, a new possibility of cross correlating HI density field from 21 cm intensity mapping(IM) to kSZ signal is discussed. HI 21 cm spectra have accurate redshift information, and are fully accessible for $z \lesssim 2$. Intensity mapping survey, rather than distinguishing individual galaxies, integrates all weak signals in a pixel, which enables it to reach high S/N and scan large sky area in much shorter time. In the following few years, there will be several experiments producing data of large sky area for redshift $\lesssim 2.5$ [11–13].

Promising as it seems, lack of large scale modes have always been a dark cloud on cross correlating IM field with large scale signals. The main challenge comes from the complicated foregrounds, which contaminate small $k_{\parallel}$ modes. Besides, in the kSZ case, the relatively low resolution and spatial loss from inteferometers will also downgrade the results. The final resolvable modes of density fields are demonstrated in Fig.1. Comparing it with the essential modes for generating kSZ in Fig.2, the deficiency of $\ell < 100$ modes for constructing velocity fields is identified as the main obstacle. Therefore an algorithm of using nonlinear tidal distortions on small scales to solve for large scale fields [14, 15] is employed in this paper. With it, velocity fields can be well reproduced. Convolving v_z with large ℓ density fields, we could at most assemble resolvable kSZ signals. This procedure is depicted at the bottom of Fig.1. Final correlation is presented against different conditions.

The paper is organized as follows: Section II introduces the way to cross correlate density fields with kSZ signals similar to [7]; Section III discusses the constraints of 21cm IM and the properties of observed fields; Section IV clarifies the important scales on density and velocity fields in terms of generating kSZ signals; Section IV describes how to use nonlinear tidal interaction to reconstruct missing large scale modes in IM fields; Results are presented in section V, while S/N is estimated in section VI; We conclude at section VII.

II. CROSS CORRELATE DENSITY FIELDS WITH KSZ MAP

The CMB temperature fluctuations caused by kSZ effect is simply an integral of the free electron momentum fields:

$$\Theta_{\rm kSZ}(\boldsymbol{n}) \equiv \frac{\Delta T_{\rm kSZ}}{T_{\rm CMB}} = -\frac{1}{c}\int d\eta g(\eta)\boldsymbol{p}_{\parallel}(\eta,\boldsymbol{n}) \; , \qquad (1)$$

where $\eta(z)$ is the comoving distance, $g(\eta) = e^{-\tau} d\tau/d\eta$ is the visibility function, τ is the optical depth for Thomson scattering, $p_{\parallel} = (1+\delta_e)v_{\parallel}$ is the momentum field parallel to the line of sight, $\delta_e = (\rho-\bar{\rho})/\bar{\rho}$ is the free electron overdensity, with $\bar{\rho}$ denotes the average density. It is assumed that electron overdensity δ_e are closely related to baryon overdensity at $z < 2$, therefore we use δ to denote both hereafter.

The direct correlation between kSZ and density field vanishes due to the cancellation of positive and negative velocity. To at most retrieve the correlation, we first reconstruct the peculiar velocity fields v_z from linear continuity equation:

$$v_z(\boldsymbol{k}) = iaHf\delta(\boldsymbol{k})\frac{k_z}{k^2} \qquad (2)$$

where a is the scale factor, $f = d\ln D/d\ln a$, $D(a)$ is the linear growth function, H is the Hubble parameter.

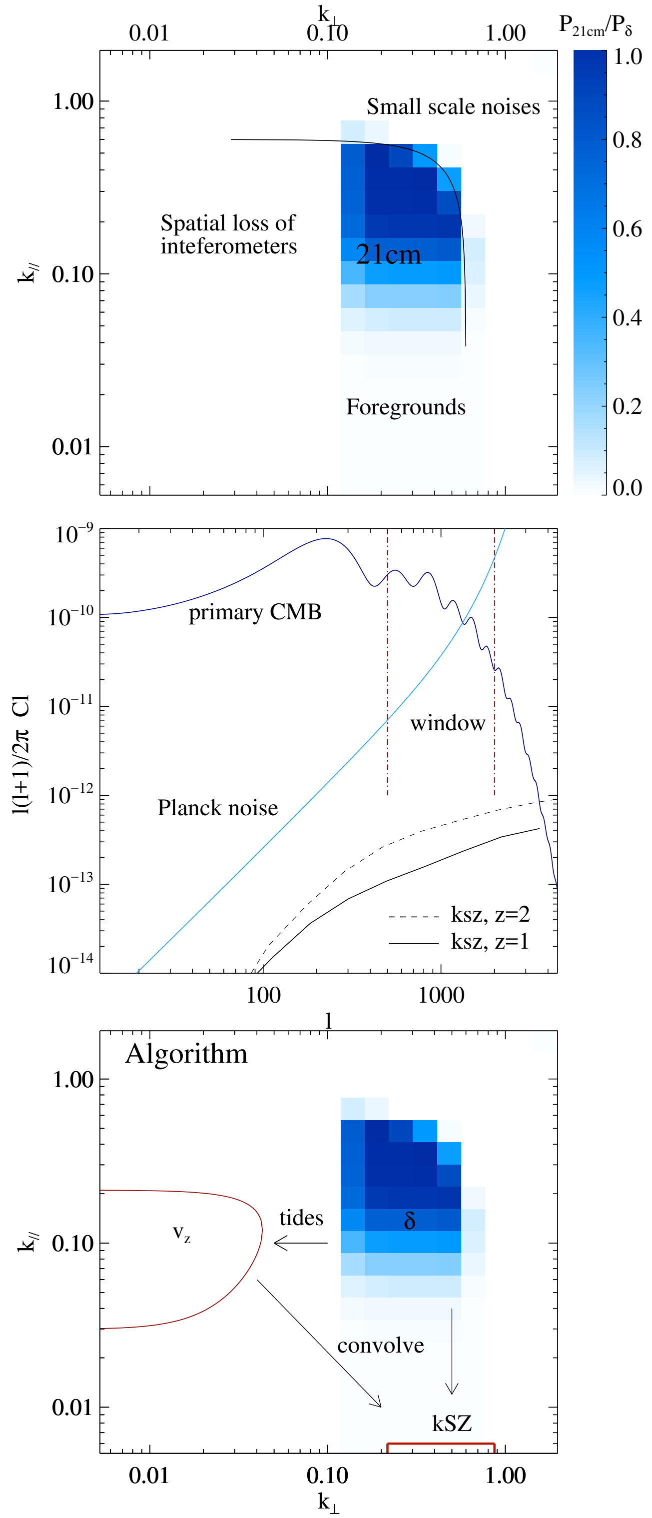

FIG. 1: (Top) Expected density fields from 21cm Intensity Mapping at $z = 1$ with CHIME, assuming high foregrounds ($R_{\parallel} = 15$ h/Mpc). (Middle) Window for kSZ measurements based on Planck noises at 217 GHz band. level of kSZ is calculated for boxes of 1.2 Gpc. (Bottom) kSZ signal comes from the cross talk of $v_z(\ell_{\rm low})$ with $\delta(\ell_{\rm high})$, with $\ell_{\rm high} - \ell_{\rm low} \sim 1000-2000$. Since large scale modes are lost in $\delta_{\rm 21cm}$, we first reconstruct it with tidal reconstruction.

We then reconstruct a 2D kSZ field with v_z and δ following Eq.(1), and quantify the tightness of correlation between reconstructed kSZ and real kSZ with a correlation coefficient r:

$$r \equiv \frac{P_{\rm recon,real}}{\sqrt{P_{\rm recon} P_{\rm real}}} \tag{3}$$

where $P_{\rm recon,real}$ is the cross power spectrum.

III. CHALLENGES FOR 21CM INTENSITY MAPPING

Ideally, this velocity reconstruction method should retrieve $> 90\%$ kSZ signals [7]. However, realistic 21cm IM experiments can only detect density fluctuations at certain scales, as illustrated in Fig.1. Three main factors lead to the loss of modes.

1. The spacial and velocity resolution of facilities.

Unlike galaxy surveys, the resolution of IM is confined to the resolution of facilities. It decides the smallest scale to be observed, and the effect could roughly be resembled with a Heaviside Function $H(k_{\rm max} - k)$.

2. Foreground noise level:

Foregrounds from Galactic emissions, extragalactic radio sources and Radio recombination lines, together with telescope noises could be three orders brighter than targeted signals[16, 17]. The process of foreground removal, taking advantage of its low spectral degrees of freedom [18], will inevitably contaminates the smooth large scale structure in radial direction. To imitate the loss, we apply a high pass filter $W(k_\parallel) = 1 - e^{-k_\parallel^2 R_\parallel^2/2}$.

3. The shortest baseline of inteferometers:

Current 21cm IM experiments are all carried on inteferometers. To avoid disturbance, two beams of a interferometer cannot be placed infinitely close. The shortest baseline length decides the largest angular scale it could probe. Structures with angular scale greater than a threshold of $\ell_{\rm min}$ will be drained out in the visibility function when cross correlating signals received from different spots. We again use a Heaviside function to assemble the effect.

Therefore, a realistic 21 cm density contrasts will appear as

$$\delta_{\rm IM}(\boldsymbol{k}) = \delta(\boldsymbol{k}) H(k_{\rm max} - k) W(k_\parallel) H(\ell - \ell_{\rm min}), \tag{4}$$

Table.I lists several representive values for different parameters based on previous observations and predictions. Fig.1 is a demonstration of density contrasts corresponding to $R_\parallel = 15$ Mpc/h, $k_{\rm max} = 0.6$ h/Mpc at $z = 1$. With this field, we construct a momentum field $p_\parallel$ following Eq.(1). As demonstrated in Fig.2, it does not cover the modes related to kSZ signals.

Actually, directly using $\delta_{\rm IM}$ of any of the parameters to reconstruct kSZ signal will yields a correlation coeffcient $r < 0.2$ with observable kSZ signals

IV. IMPORTANT SCALES FOR KSZ SIGNALS

To understand the indispensable $\boldsymbol{k}$ for δ in reconstructing kSZ signals, the first step is to clarify which angular scale of

	z=1		z=2	
	high foreground	low foreground	high foreground	low foreground
$R_\parallel$ Mpc/h [a]	15	60	10	40
	CHIME	HIRAX	CHIME	HIRAX
$k_{\rm max}$ h/Mpc [b]	0.6	1.2	0.4	0.8
$\ell_{\rm min}$ [c]	300			

[a]Foreground: smear $k_z \lesssim 0.08, 0.02, 0.12, 0.03$ h/Mpc respectively. Parameters based on [19–21]

[b]Small scale noises: based on CHIME[11] and HIRAX[13] with 100 m and 200 m longest baseline respectively.

[c]Spatial loss of inteferomenter: assuming shortest baseline of 20 m.

TABLE I: Parameters related to resolvable modes in 21cm IM

the kSZ we are interested in. As demonstrated in Fig.1, the kSZ effect is too faint to be distinguished until primary CMB starts to fade away, which is roughly $\ell > 500$. It is possible to select a frequency band with thermal SZ signal negligible, then the dominant factor on high ℓ will be the CMB facility noises. Consider existing Planck [22] data at 217 GHz, $\ell \sim 500 - 3000$ will be the visible window for kSZ signal. The window could be extended to higher frequency with ACTpol and CMB-S4.

The next step is to understand what role each scale plays in generating kSZ signal at $\ell \sim 500 - 3000$. Write Eq.(1) in Fourier space. Given $g(\eta)$ varies slowly. $\Theta(\boldsymbol{\ell})$ is propotional to the $k_z = 0$ mode of the momentum field, as marked in Fig.2,

$$\begin{aligned} \Theta(\boldsymbol{\ell}) \;&\propto\; p_\parallel(k_x\chi, k_y\chi, 0) \\ &\propto\; \int d^3k'\, \delta(\boldsymbol{\ell}/\chi - \boldsymbol{k}'_\perp, k'_\parallel) v_z(\boldsymbol{k}') \end{aligned} \tag{5}$$

The convolution of δ and v_z indicates the signal comes from the cross talk of $\boldsymbol{\ell}/\chi - \boldsymbol{k}'_\perp$ and $\boldsymbol{k}_\perp$, sum over all k'.

Since $v_z \propto k_z/k^3$, it drops fast at small scales. Boldly analogize v_z to a Dirac delta function $\delta^D(\boldsymbol{k}')$, $\Theta(\boldsymbol{\ell})$ will reduce to $\propto \delta(\boldsymbol{\ell}/\chi, 0) v_z(0,0)$, with integration of other k' negligible due to the faintness of $v_z(k' \neq 0)$. Adapt the analogy into reality, where $v_z(\boldsymbol{k})$ is not as sharp as δ^D, and the peak will be more close to ($k_\perp$,$k_\parallel$)=(0.01,0.1) h/Mpc rather than (0,0), we will see that most of the kSZ signals are generated from the cross talk between the part of $v_z(\boldsymbol{k})$ with k in a small ball surrounding (0.01,0.1) h/Mpc and the part of $\delta(k)$ with k close to $\delta(\boldsymbol{\ell}/\chi, 0.1)$ h/Mpc. This is demonstrated in Fig.2. Comparing it with Fig.1, we notice that while the essential modes for δ are partly resolved, the large scale information dominating v_z is almost completely drained out in 21 IM fields.

Therefore, the primary task to derive the cross correlation between kSZ and 21cm IM fields is to reconstruct the large scale modes for v_z.

V. COSMIC TIDAL RECONSTRUCTION

Till now only linear theories are considered in reconstruction, however, to extract the lost large scale information, we need to consider couplings between different scales in nonlinear theories. While there are a great variety of nonlinear effects, identifying a single one will help conduct clean reconstruction.

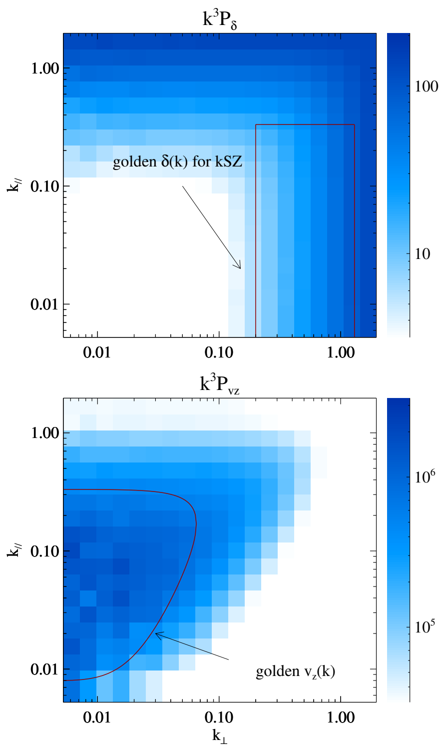

FIG. 2: The variance $2\pi^2\Delta^2 \equiv k^3P$ indicate how Fourier modes of different scales contribute to real space fields, i.e. $\delta(\boldsymbol{x})$ and $v_z(\boldsymbol{x})$. Golden modes for kSZ at $\ell \sim 500-3000$ are marked out.

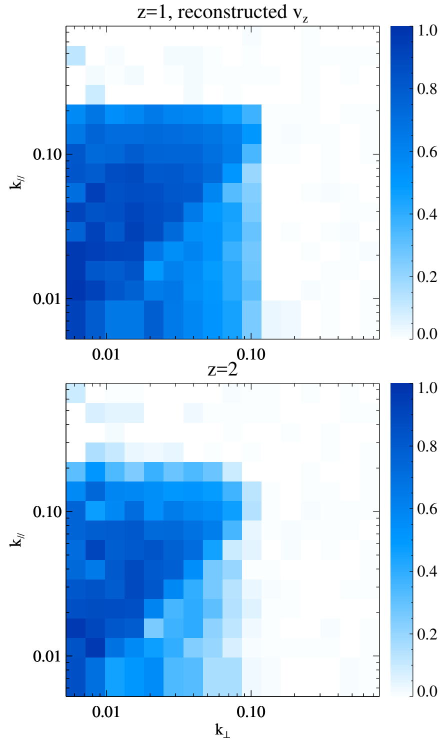

FIG. 3: The correlation coefficient between reconstructed v_z and actual v_z assuming a baseline of 100 m, foregrounds seriously contaminate k_z below $\sim$ 0.08 h/Mpc and $\sim$ 0.12 h/Mpc at $z=1\&2$, respectively.

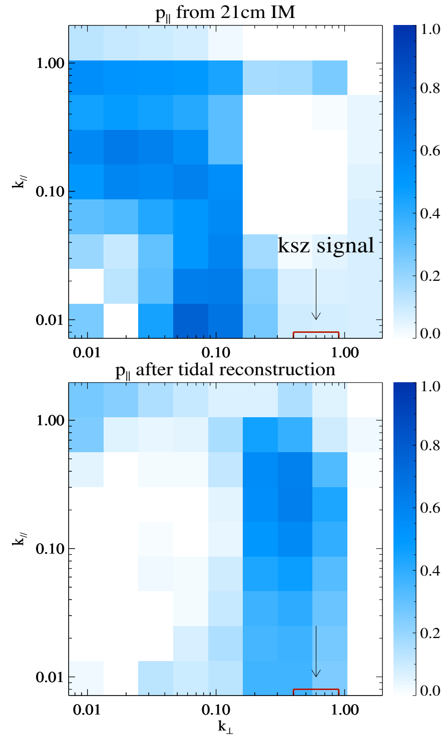

FIG. 4: The correlation coefficient for $p_{\|} = (1+\delta)v_z$ before and after tidal reconstruction. The kSZ is roughly $p_{\|}$ integrated over line of sight, corresponding to $k_z = 0$ modes.

Here, we present an algorithm to employ tidal coupling to solve for large scale structures [14, 15].

The evolution of small scale structure is modulated by large scale tidal force. Consider only the anisotropic influence from tidal force, the generated distortions on matter power spectrum will be

$$\delta P(\boldsymbol{k},\tau)|_{t_{ij}} = \hat{k}^i\hat{k}^j t_{ij}^{(0)} P_{1s}(k,\tau) f(k,\tau) \tag{6}$$

where $P_{1s}(k,\tau)$ is the linear power spectrum; $f(k) = 2\alpha(\tau) - \beta(\tau) d\ln P/d\ln k$ is the tidal coupling function, with α and β parameters related to linear growth funcion [15]. $(\alpha,\beta) = (0.6, 1.3)$ and $(0.4, 0.9)$ for $z=1$ and $z=2$ respectively. t_{ij} is the tidal force tensor, which is symmetric and traceless and hence can be decomposed into five components

$$t_{ij} = \begin{pmatrix} \gamma_1 - \gamma_z & \gamma_2 & \gamma_x \\ \gamma_2 & -\gamma_1 - \gamma_z & \gamma_y \\ \gamma_x & \gamma_y & 2\gamma_z \end{pmatrix}. \tag{7}$$

Therefore, from spatial dependence of the distortions $\delta P(\boldsymbol{k},\tau)$, we could solve for different components of t_{ij}. And since tidal forces are related to second derivative of large scale gravitational potential Φ_L,

$$t_{ij} = \partial_i\partial_j\Phi_L - \nabla^2\Phi_L\delta_{ij}^D/3/, \tag{8}$$

where δ_{ij}^D is the Dirac function which equals 1 when $i=j$ and equals 0 otherwise.

Different components of t_{ij} is related to different k modes of the large scale density contrast $\kappa_{3\mathrm{D}}$.

$$\kappa_{3\mathrm{D}} \sim \nabla^2\Phi_L = \frac{3}{2}\nabla^{-2}\partial_i\partial_j t_{ij} \tag{9}$$

Notice that $f(k,\tau)$ increases with k in the interested scales, indicating the distortions are more manifest on small scales. This explains the feasibility of using existing high k modes in 21cm IM fields to extract low k modes.

VI. SIMULATIONS AND RESULTS

To test the algorithm, six N-body simulations are performed with the CUBEP^{3}M code [23], each evolving 1024^3 particles in a $(1.2\mathrm{Gpc}/h)^3$ box. Simulation parameters are set as: Hubble parameter $h=0.678$, baryon density $\Omega_b = 0.049$, dark matter density $\Omega_c = 0.259$, amplitude of primordial curvature power spectrum $A_s = 2.139\times10^{-9}$ at $k_0 = 0.05\ \mathrm{Mpc}^{-1}$ and scalar spectral index $n_s = 0.968$.

Simulated density and velocity fields at $z=1,2$ are output and used to generate kSZ signal.

To avoid manipulating noises, we perform tidal reconstruction on most conservative estimates, i.e. $R_{\|} = 15$ Mpc/h,

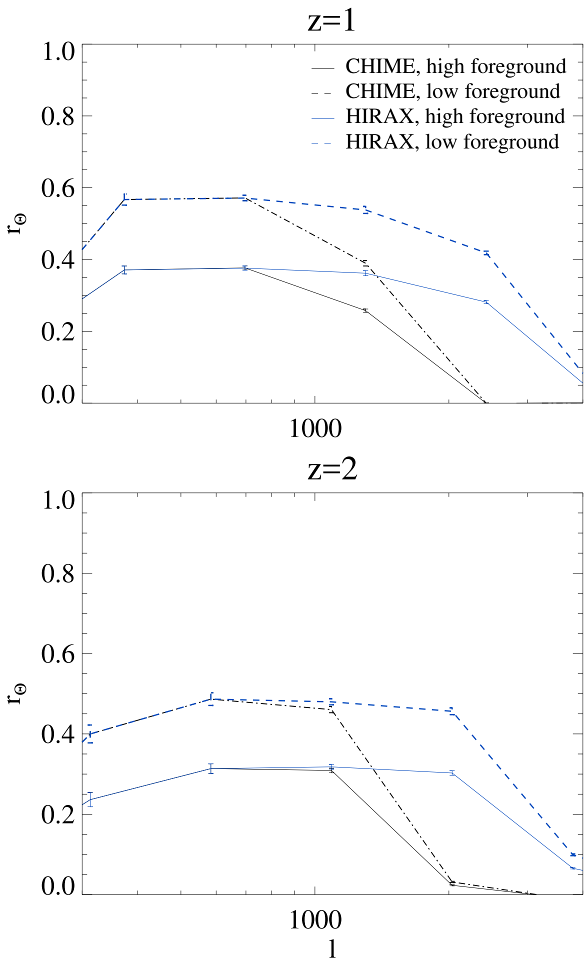

FIG. 5: The correlation coefficient r between real kSZ $P_{\rm real}$ and 21cm IM reconstructed kSZ $P_{\rm recon}$.

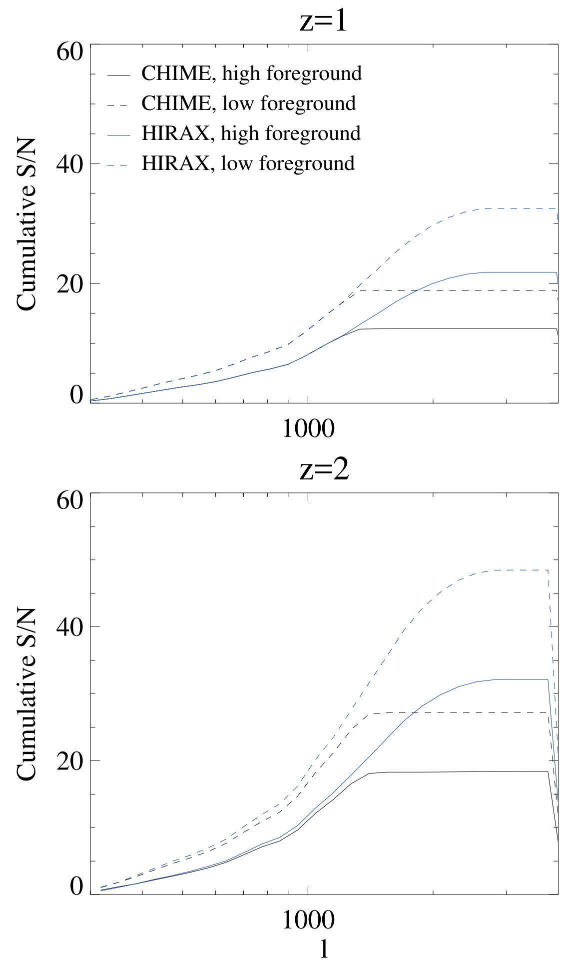

FIG. 6: Cumulative S/N, assuming Planck noise at 217 GHz, $f_{sky} = 0.8$.

$k_{\rm max} = 0.6$ h/Mpc, $\ell_{\rm min} = 200$ for $z = 1$; and $R_{\|} = 10$ Mpc/h, $k_{\rm max} = 0.4$ h/Mpc, $\ell_{\rm min} = 200$ for $z = 2$. Refer to Table.I, top of Fig.1 and Chapter.III for meaning of the parameter.

The cross correlation between reconstructed v_z and actual v_z are demonstrated in Fig.3. Important modes for velocity fields (within redline of Fig.2 lower label) are well extracted with correlations greater than 0.7.

Combining reconstructed velocity field with density fields of different conditions, we get the reconstructed kSZ signals. Their correlation coefficients with exact kSZ are demonstrated in Fig.5. Even with identical tidal reconstructed velocity field, better foreground techneque can improve the correlation coefficient by 0.2. If the foreground is removed clean enough for more modes to be used in tidal reconstruction procedure, the improvement will be more notable. Resolution of facility will improve the reconstruction on higher ℓ, consisting with previous analysis.

VII. STATISTICAL ERROR AND S/N

Consider primary CMB and facility noises, the chances to seperate kSZ signal from statistical errors could be estimated with:

$$\begin{aligned} \frac{S}{N} &= \frac{C_\ell}{\Delta C_\ell} \\ &\simeq r\sqrt{(2\ell+1)\Delta l f_{\rm sky}}\sqrt{\frac{C_\ell^{{\rm kSZ},\Delta z}}{C_\ell^{\rm CMB}+C_\ell^{\rm kSZ}+C_\ell^{{\rm CMB},N}}}, \end{aligned} \tag{10}$$

where $C_\ell^{\rm CMB}$ is the angular power spectrum of primary CMB ; $C_\ell^{\rm CMB,N}$ indicates the facility noises; $C_\ell^{{\rm kSZ},\Delta z}$ is the kSZ signal from a certain redshift bin; r is the correlation coefficients from Eq.(3); $f_{\rm sky}$ is the percent of sky area covered by both surveys.

In our case, $C_\ell^{\rm CMB}$ is calculated from CAMB [24]. $C_\ell^{\rm CMB,N}$ is estimated with Planck data [22] at 217GHz, with sensitivity per beam solid angle $\sigma_{p,T} = 8.7\mu K_{\rm CMB}$ and effective beam FWHM $\theta_{\rm FWHM} \sim 5'$. We choose $f_{\rm sky} = 0.8$ according to claimed 21 cm IM survey area. $C_\ell^{{\rm kSZ},\Delta z}$ is calculated within two bins of size 1200 Mpc/h, centered at redshift 1 & 2, respectively.

The cumulative S/N is demonstrated in Fig.6. The low correlation in $z = 2$ is compensated by the high electron density and the overall S/N could well reach 50 with HIRAX.

With noise level of Planck, the resolution of HIRAX already cover most important ℓ.

VIII. CONCLUSION

In this paper, we discuss the possibility of cross correlating kSZ signal with 21 cm intensity mapping to study baryon distributions. All the calculations are based on ongoing experiment condition and realistic noise scales. A holographic way of cross correlation is applied. Nonlinear tidal coupling of different scales are employed to compensate for lost large scale modes. The method is essentially about studying four point correlation function $< \delta\,\delta\,\delta\,T >$, but in a controlled and well-understood way: using small scale distortions on power spectrum $< \delta_s \delta_s >$ to reconstruct large scale modes δ_L and hence v_z, and then convolve density and velocity fields $< \delta_s v_z >$ to mimic kSZ signal.

With existing Planck data, it is reasonable to expect at least ~ 15 S/N with data from CHIME, and more optimistic estimates will yield 50 S/N for redshift 2 with HIRAX. The main obstacle for optimal correlation is lack of low k_z high $k_\perp$ data due to foregrounds. This leads to information waste in the reconstructed velocity field. However, data from weak lensing, photo-z galaxy surveys, which contains only large scale structure in z direction, may compensate for that.

This method is promising for its feasibility and model independence. CHIME already starts to collect data, and HIRAX is also in a close flight. It is reasonable to expect it to be tested within five years. Moreover, the method does not rely on assumptions about velocity fields or interstellar medium conditions. Less misunderstanding will appear while interpreting results. It is reasonable to expect it to be a new reliable attemp to study baryon distributions up to redshift 2 or higher. And the unique property of 21cm IM of having both large sky coverage and accurate redshift information offers a eye to look at diffusive baryon at the angular scale of $\ell \sim 1000 - 2000$, which is of larger scale than all the other similar methods proposed. This will foster the understanding of feedbacks at the scale of galaxy clusters and filaments and hence structure evolutions.

IX. ACKNOWLEDGE

We acknowledge discussions Wenkai Hu, Tianxiang Mao and Jiawei Shao. The simulations were performed on the BGQ supercomputer at the SciNet HPC Consortium. SciNet is funded by: the Canada Foundation for Innovation under the auspices of Compute Canada; the Government of Ontario; the Ontario Research Fund – Research Excellence; and the University of Toronto. Research at the Perimeter Institute is supported by the Government of Canada through Industry Canada and by the Province of Ontario through the Ministry of Research & Innovation. The Dunlap Institute is funded through an endowment established by the David Dunlap family and the University of Toronto.

[1] U.-L. Pen, ApJ **510**, L1 (1999), astro-ph/9811045.

[2] A. M. Sołtan, A&A **460**, 59 (2006), astro-ph/0604465.

[3] R. A. Sunyaev and Y. B. Zeldovich, Comments on Astrophysics and Space Physics **4**, 173 (1972).

[4] R. A. Sunyaev and I. B. Zeldovich, MNRAS **190**, 413 (1980).

[5] E. T. Vishniac, ApJ **322**, 597 (1987).

[6] N. Hand, G. E. Addison, E. Aubourg, N. Battaglia, E. S. Battistelli, D. Bizyaev, J. R. Bond, H. Brewington, J. Brinkmann, B. R. Brown, et al., Physical Review Letters **109**, 041101 (2012), 1203.4219.

[7] J. Shao, P. Zhang, W. Lin, Y. Jing, and J. Pan, MNRAS **413**, 628 (2011), 1004.1301.

[8] M. Li, R. E. Angulo, S. D. M. White, and J. Jasche, MNRAS **443**, 2311 (2014), 1404.0007.

[9] J. C. Hill, S. Ferraro, N. Battaglia, J. Liu, and D. N. Spergel, ArXiv e-prints (2016), 1603.01608.

[10] S. Ferraro, J. C. Hill, N. Battaglia, J. Liu, and D. N. Spergel, ArXiv e-prints (2016), 1605.02722.

[11] K. Bandura, G. E. Addison, M. Amiri, J. R. Bond, D. Campbell-Wilson, L. Connor, J.-F. Cliche, G. Davis, M. Deng, N. Denman, et al., in *Society of Photo-Optical Instrumentation Engineers (SPIE) Conference Series* (2014), vol. 9145 of *Society of Photo-Optical Instrumentation Engineers (SPIE) Conference Series*, p. 22, 1406.2288.

[12] Y. Xu, X. Wang, and X. Chen, ApJ **798**, 40 (2015), 1410.7794.

[13] http://www.acru.ukzn.ac.za/ hirax/.

[14] U.-L. Pen, R. Sheth, J. Harnois-Deraps, X. Chen, and Z. Li, ArXiv e-prints (2012), 1202.5804.

[15] H.-M. Zhu, U.-L. Pen, Y. Yu, X. Er, and X. Chen, ArXiv e-prints (2015), 1511.04680.

[16] T. Di Matteo, B. Ciardi, and F. Miniati, MNRAS **355**, 1053 (2004), astro-ph/0402322.

[17] K. W. Masui, E. R. Switzer, N. Banavar, K. Bandura, C. Blake, L.-M. Calin, T.-C. Chang, X. Chen, Y.-C. Li, Y.-W. Liao, et al., ApJ **763**, L20 (2013), 1208.0331.

[18] E. R. Switzer, T.-C. Chang, K. W. Masui, U.-L. Pen, and T. C. Voytek, ApJ **815**, 51 (2015), 1504.07527.

[19] K. W. Masui, E. R. Switzer, N. Banavar, K. Bandura, C. Blake, L.-M. Calin, T.-C. Chang, X. Chen, Y.-C. Li, Y.-W. Liao, et al., ApJ **763**, L20 (2013), 1208.0331.

[20] E. R. Switzer, K. W. Masui, K. Bandura, L.-M. Calin, T.-C. Chang, X.-L. Chen, Y.-C. Li, Y.-W. Liao, A. Natarajan, U.-L. Pen, et al., MNRAS **434**, L46 (2013), 1304.3712.

[21] J. R. Shaw, K. Sigurdson, M. Sitwell, A. Stebbins, and U.-L. Pen, Phys. Rev. D **91**, 083514 (2015), 1401.2095.

[22] Planck Collaboration, R. Adam, P. A. R. Ade, N. Aghanim, M. Arnaud, M. Ashdown, J. Aumont, C. Baccigalupi, A. J. Banday, R. B. Barreiro, et al., ArXiv e-prints (2015), 1502.01587.

[23] J. Harnois-Déraps, U.-L. Pen, I. T. Iliev, H. Merz, J. D. Emberson, and V. Desjacques, MNRAS **436**, 540 (2013), 1208.5098.

[24] A. Lewis, A. Challinor, and A. Lasenby, Astrophys. J. **538**, 473 (2000), astro-ph/9911177.